Efficient Reduction of Graphite Oxide by Sodium Borohydride and Its Effect on Electrical Conductance

By *Hyeon-Jin Shin, Ki Kang Kim, Anass Benayad, Seon-Mi Yoon, Hyeon Ki Park, In-Sun Jung, Mei Hua Jin, Hae-Kyung Jeong, Jong Min Kim, Jae-Young Choi,** and *Young Hee Lee**

The conductivity of graphite oxide films is modulated using reducing agents. It is found that the sheet resistance of graphite oxide film reduced using sodium borohydride ($NaBH_4$) is much lower than that of films reduced using hydrazine (N_2H_4). This is attributed to the formation of C–N groups in the N_2H_4 case, which may act as donors compensating the hole carriers in reduced graphite oxide. In the case of $NaBH_4$ reduction, the interlayer distance is first slightly expanded by the formation of intermediate boron oxide complexes and then contracted by the gradual removal of carbonyl and hydroxyl groups along with the boron oxide complexes. The fabricated conducting film comprising a $NaBH_4$-reduced graphite oxide reveals a sheet resistance comparable to that of dispersed graphene.

1. Introduction

Graphite oxide (GO) has recently attracted much interest for several reasons. GO has been reported to have a high dispersion stability at pH values over 9,[1] enabling the fabrication of films possessing large surface areas. GO films can be reduced to obtain a graphene-like sheet. Several reduction techniques, such as thermal or chemical reduction, have been used to convert insulating GOs to conducting graphene-like layers.[2–11] Thermal reduction has been highly effective in producing graphene-like films with a C:O ratio of up to 9 and minimal defect formation.[2,3] However, this approach is limited by the choice of substrate; i. e., typical transparent plastic substrates cannot be used due to its low glass transition temperature. On the other hand, chemical reduction is very simple, but it usually generates graphene-like film exhibiting a relatively low C:O ratio and a considerable amount of residual functional groups, resulting in a highly resistive film.[4–9] In general, the reduction mechanism by chemical reducing agents has been unclear. The production of graphene by GO reduction presumably has a high activation barrier, which is supported by the improved reduction achieved by combining chemical and thermal techniques.[10,11] Even though oxygen atoms are mostly effectively removed by combined reduction techniques, some remaining oxygen atoms and additional functional groups introduced during chemical reduction may result in the scattering of electrons, increasing the sheet resistance of the film. Therefore, it is necessary to develop a more effective chemical reduction method to produce graphene-like film with high electrical conductivity.

Up to now, many researchers have used hydrazine (N_2H_4) to reduce GO. Unfortunately, this chemical approach gave rise to high sheet resistance, which would be too high for actual applications.[10–12] Furthermore, N_2H_4 is toxic; it has been suggested that some C–N groups incorporated during reduction remain in the sample.[4–8] However, a direct correlation between the presence of these functional groups and the sheet resistance has not been observed.

In this study, we introduce the use of the reducing agent, sodium borohydride ($NaBH_4$), in elucidating the underlying reduction mechanism of GO. A similar reduction of N_2H_4 was also performed for comparison. The C:O ratio and information regarding any functional groups of the reduced GO (RGO) were investigated by X-ray photoelectron spectroscopy (XPS). The formation of intermediate complexes, the interlayer distances, and the work function of the RGO were systematically investigated as functions of molar concentration of the reducing agent by X-ray diffraction (XRD) and ultraviolet photoelectron (UPS), UV-vis, and Raman spectroscopy. Electrical properties were characterized by current–voltage, *I–V*, measurements. Application of RGO as transparent conducting films demonstrated that the high sheet resistance of N_2H_4-reduced GO arises from the presence of C–N groups, which was confirmed by XPS studies.

[*] Dr. J.-Y. Choi, H.-J. Shin, Dr. A. Benayad, S.-M. Yoon, I.-S. Jung, Dr. J. M. Kim
Display Lab, Analytical Engineering Center
Samsung Advanced Institute of Technology
Yongin, Gyeonggi-do 446-712 (Korea)
E-mail: jaeyoung88.choi@samsung.com
Prof. Y. H. Lee, H.-J. Shin, Dr. K. K. Kim, H. K. Park, M. H. Jin, Dr. H.-K. Jeong
BK21 Physics Division
Sungkyunkwan Advanced Institute of Nanotechnology
Center for Nanotubes and Nanostructured Composites
Sungkyunkwan University
Suwon, Gyeonggi-do 440-746(Korea)
E-mail: leeyoung@skku.edu

DOI: 10.1002/adfm.200900167

2. Results and Discussion

2.1. Comparison between the Reducing Effect of N_2H_4 and $NaBH_4$

N_2H_4 has been used by several groups as a reducing agent to improve the conductivity of GO film.[4–8,10–11] Although chemical reduction gave rise to improvements in film conductivity, the underlying reduction mechanism has not been clearly understood. For this purpose, we used the two reducing agents, N_2H_4 and $NaBH_4$, without thermal reduction. Table 1 summarizes the differences of the RGO films in terms of elemental composition and resulting sheet resistance, given in $k\Omega\ sq^{-1}$ where sq represents square. The atomic ratio of carbon and oxygen was obtained by taking the ratio of C 1s to O1s peak areas in XPS spectra (Fig. S1, Supporting Information). This ratio represents the degree of reduction, and it could be altered varying the dipping time of the sample in the desired solution. In order to directly compare the effects of the reducing agent, sheet resistance was measured for RGO films having similar C–O composition. In both cases, reduced sheet resistance was observed with decreasing oxygen content. We emphasize here that the sheet resistance of $NaBH_4$-reduced GO films was much lower than that of N_2H_4-reduced films of similar C–O composition. The decrease of the heterocarbon component in the C 1s peak, such as that arising from hydroxyl (C−O), epoxy (C−O−C), and carbonyl (C=O, O−C=O) groups, was consistent with the increase of the C:O ratio in $NaBH_4$-reduced GO films. It is of note that in N_2H_4-reduced films, the heterocarbon component of the C 1s peak that includes carbon in C−N groups changed slightly with the dipping times in spite of the gradual increase of the C:O ratio.[4,5] Also, the N 1s peak near 399.8 eV was visible, and an increase in N 1s peak intensity was observed with increasing C:O ratio (Table S1 and Fig. S2, S3, Supporting Information). This implies that the C−N component should increase with increasing dipping times. We interpret these results to indicate that N_2H_4 treatment results in a continuous accumulation of nitrogen atoms and a removal of oxygen atoms in the GO films. Generally, while N_2H_4 reduction is known to form hydrocarbons from carbonyl groups,[13] $NaBH_4$-reduction forms residual hydroxyl functional groups.[14] Therefore, N_2H_4 is expected to be a better reducing agent than $NaBH_4$ for GO. Nevertheless, in our work, the formation of hydrocarbons from carbonyl functional groups in GO by N_2H_4-reduction was not effective, and resulting RGO films had some C−N groups. Compounds containing nitrogen have been known as n-type chemical dopants.[15–17] Therefore, the nitrogen complex of N_2H_4 behaves as a donor compensating p-type holes.[18–20] This resulted in the conclusion that use of 10 mM $NaBH_4$ as the reducing agent is more beneficial than 50 mM N_2H_4 in lowering sheet resistance. Nevertheless, the sheet resistance of $NaBH_4$-reduced GO was still relatively high due to a low C:O ratio in comparison to that of graphite. In order to further decrease sheet resistance, the molar concentration of $NaBH_4$ was increased to 150 mM. In this case, dipping times were shortened to two hours to avoid the self-oxidation of $NaBH_4$ in water.

2.2. XRD Patterns, UV-Vis Spectra, and Raman Spectra of $NaBH_4$

Figure 1 shows the XRD patterns of films reduced using various molar concentrations of $NaBH_4$. The interlayer distance obtained from the (002) peak was 3.38 Å ($2\theta = 26.4^\circ$) in graphite. This was markedly expanded to 8.27 Å ($2\theta = 10.7^\circ$) with oxidation to form GO (Fig. 1, top pattern).[21,22] The large interlayer distance has been attributed to the formation of hydroxyl, epoxy, and carboxyl groups. With reduction, the interlayer distance is expected to

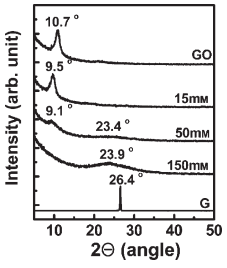

Figure 1. XRD patterns of GO, graphite (G), and reduced GOs obtained using various molar concentrations of $NaBH_4$.

Table 1. Sheet resistance and elemental composition of reduced GO films using $NaBH_4$ or N_2H_4, as the reducing agents.

$NaBH_4$ (10 mM)			N_2H_4 (50 mM)			
XPS		Sheet resistance [$k\Omega\ sq^{-1}$]	XPS			Sheet resistance [$k\Omega\ sq^{-1}$]
Total elemental C:O ratio	Heterocarbon component of C 1s peak [%]		Total elemental C:O ratio	Heterocarbon component of C 1s peak [%]	N 1s peak intensity [%]	
2.8 [a]	74.1	–	2.8 [a]	74.1	–	–
4.3	27.9	–	3.9	26.4	1.3	69 000
4.9	16.2	79	4.5	19.0	2.1	12 000
5.3	13.4	59	5.0	18.6	2.6	3 460
			6.2	14.5	2.4	780

[a] GO sample.

contract due to the removal of such functional groups. The interlayer distance, however, was further expanded to 9.31 Å ($2\theta = 9.5^\circ$) by 15 mM $NaBH_4$ reduction. Further increasing the molar concentration of the reducing agent resulted in a slightly expanded interlayer distance of 9.72 Å ($2\theta = 9.1^\circ$), and the intensity of the (002) peak was significantly reduced, while a small bump appeared near 3.80 Å ($2\theta = 23^\circ$). Using 150 mM of the reducing agent, the peak of the large interlayer distance disappeared completely and a broad peak near 3.73 Å ($2\theta = 23.9^\circ$) became visible. This implied that most of the functional groups were removed, and it should be noted that XRD pattern was similar to that of graphite. The peak, however, was rather broad and slightly different from that observed in the graphite XRD pattern.

Figure 2a shows the C 1s peak, which consists of two main components arising from C−O (hydroxyl and epoxy, ~286.5 eV) and C=O (carbonyl, ~288.3 eV) groups and two minor components from C=C/C−C (~284.6 eV) and O−C=O (carboxyl, ~290.3 eV) groups.[21–24] Using 15 mM $NaBH_4$, the spectra indicated that carbonyl groups were first transformed into C−O bonds (286.1 eV; hydroxyl groups), while some carboxyl groups were partially removed. Using 50 mM $NaBH_4$, all of the carbonyl groups were nearly removed, and the C−O bonds were reduced as well.[4,5,21,22] No significant reduction of the oxygen-related functional groups was observed at the higher $NaBH_4$ concentration of 150 mM. Some amount of oxygen atoms was retained in the film even after treatments involving high molar concentrations. Areas of the contributing peaks are listed in Table 2. The presence of epoxy and hydroxyl groups in GO and disappearance of such functional groups in RGO were also confirmed by ^{13}C NMR spectroscopy (Fig. S4, Supporting Information). It is of particular note that boron oxide complexes were visible in films treated with 15 mM $NaBH_4$ (Fig. 2f). These complexes were not noticed in samples treated using other molar concentrations. The presence of boron oxide complexes can account for why the interlayer distance expanded further in samples reduced using 15 mM $NaBH_4$ (Fig. 1). At low molar concentration of $NaBH_4$, boron oxides formed and interacted with functional groups of the GO, slightly expanding the interlayer distance. Higher $NaBH_4$ concentrations resulted in the removal of the boron oxide complexes along with other functional groups in GO, and thus, the interlayer distance was reduced.

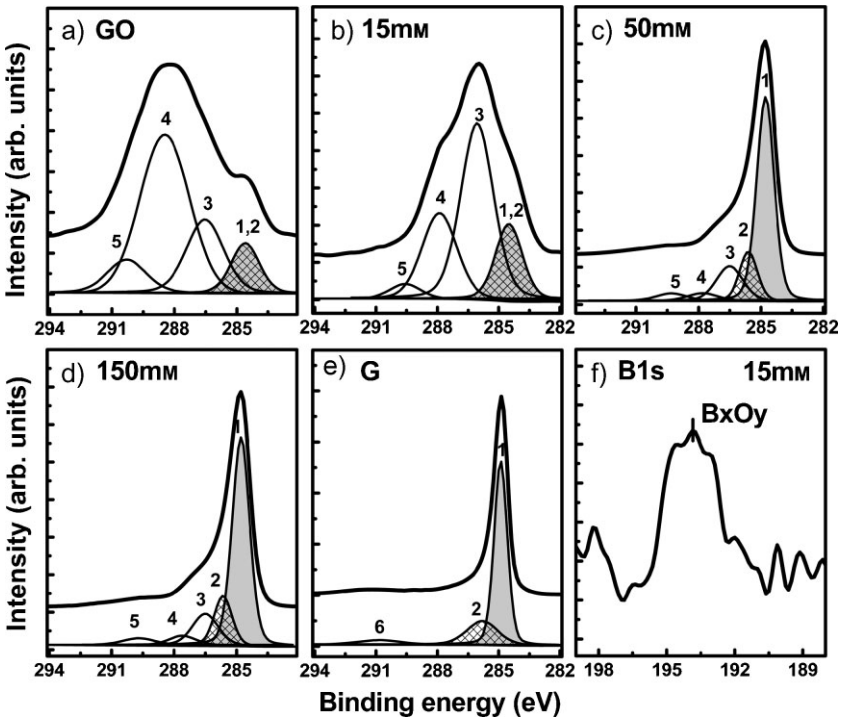

Figure 2. The C 1s peak in the XPS spectra of GO (a), reduced GO obtained using 15 (b), 50 (c), and 150 mM $NaBH_4$ (d), and graphite (f); the curve was fitted considering the following contributions: C=C (sp^2; peak 1), C−C (sp^3; peak 2), C−O/C−O−C (hydroxyl and epoxy groups; peak 3), C=O (carbonyl groups; peak 4), O−C=O (carboxyl groups; peak 5), and π-π* (peak 6). e) The B 1s peak in the XPS spectrum of the reduced GO obtained using 15 mM $NaBH_4$.

Figure 3a shows the UV-vis spectra of GO and three RGO films. The absorption peak of GO around 230 nm was gradually red-shifted towards 260 nm in films treated with higher concentrations of $NaBH_4$. The peaks of GO at ~300 and 360 nm evidently disappeared. This indicated the formation of highly conjugated structure like that of graphite.[25] The formation of defects were monitored by the ratio of the intensities of the D and G bands (D:G) in the Raman spectra, as shown in Figure 3b and 3c. The number of defects slightly increased at low concentrations of the reducing agent, but a drastic increase was

Table 2. The C 1s peak position and the relative atomic percentage of various functional groups in GO, graphite, and RGO films obtained using different molar concentration of $NaBH_4$.

	Fitting of the C 1s peak Binding energy [eV] (relative atomic percentage [%])					
	C=C (sp^2)	C−C (sp^3)	C−O/C−O−C	C=O	O−C=O	π-π*
GO	284.6 (11.3)		286.5 (21.7)	288.3 (56.8)	290.3 (10.2)	
15 mM	284.6 (17.8)		286.1 (51.6)	288.1 (25.8)	289.6 (5.1)	
50 mM	284.8 (61.6)	285.6 (14.8)	286.5 (15.0)	287.8 (3.9)	289.3 (4.7)	
150 mM	284.8 (63.3)	285.6 (15.0)	286.5 (13.8)	287.6 (4.2)	289.6 (3.6)	
Graphite	284.8 (77.0)	285.7 (19.3)				291.1 (3.7)

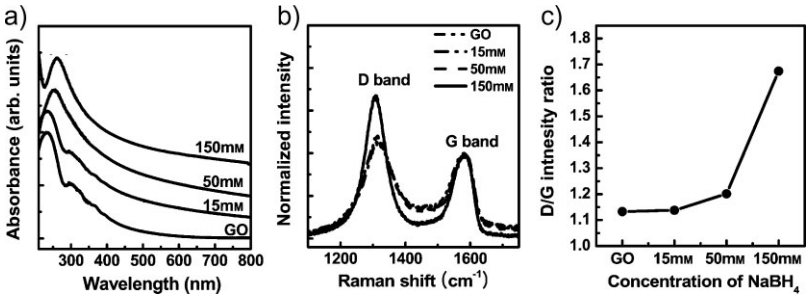

Figure 3. a) UV-vis and b) Raman spectra of GO and RGO films and c) the dependence of the D:G ratio on the $NaBH_4$ concentration in the RGO films.

observed when 150 mM of $NaBH_4$ was used; this observation is contrary to the general belief that defects should decrease during the reduction process by the removal of oxygen atoms followed by the formation of double bonds.

2.3. Structure-Related Electrical Properties of Reduced GO

The electronic properties of RGO are closely related to its structural properties. Figure 4a shows the conductivity and C:O ratio as a function of the molar concentration of $NaBH_4$. The behavior of the conductivity and C:O ratio were very similar to each other the $NaBH_4$ concentration was increased. Conductivity of the film was directly related to the oxygen content. Complete removal of residual oxygen content even when using high $NaBH_4$ concentrations was the key factor in further reducing the sheet resistance. The presence of oxygen atoms also affects the electronic density of states, as shown in Figure 4b. An oxygen-related peak (O 2s) appeared near 27.0 eV in the density of states of GO. This peak was retained even when high $NaBH_4$ concentrations were used to reduce the films, enabling a good contrast with the valence band structure of graphite. Furthermore, the intensity of the GO π states less than 5 eV from the Fermi level did not fully recover to similar values as observed in graphite even when using high concentrations of the reducing agent. As shown in Table 3, the C–O composition of the RGO obtained using 150 mM $NaBH_4$ was very different from that of graphite. Therefore, the conductivity of RGO did not reach the value typically observed for graphite. Table 3 also shows how the work function, as measured by UPS, varied in the different samples. The work function gradually increased with the C:O ratio; as expected, it approached that of graphite.

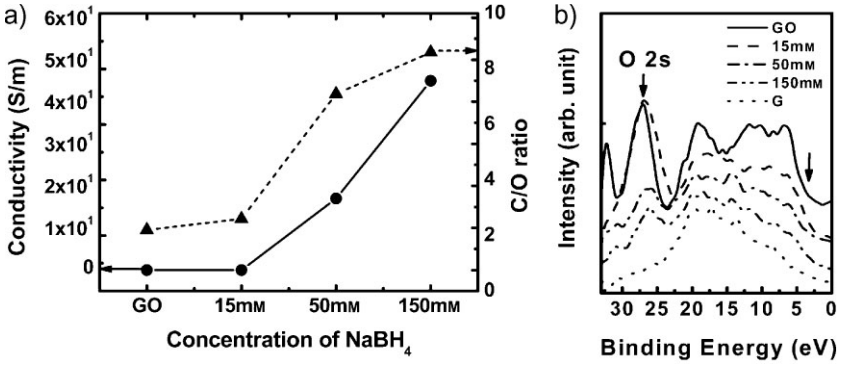

Figure 4. a) Dependence of the conductivity on the C:O ratio and b) the valence band structure of RGO films obtained using various concentrations of $NaBH_4$.

2.4. Characteristics of RGO as a Transparent Conducting Film

Figure 5 shows how sheet resistance varied with respect to the transmittance for different film thicknesses. Our $NaBH_4$-reduced GO films exhibited the lowest sheet resistance compared to all other RGO sheets, which were reduced using N_2H_4.[10,11] For instance, at a transmittance of 83%, the sheet resistance of our RGO film was 5.2 kΩ sq^{-1} (Table 4); this is significantly smaller than 1500 MΩ sq^{-1} or 100 kΩ sq^{-1}, which were observed for samples that had been additionally thermally annealed at 200 °C under nitrogen (or vacuum) in spite of a 3% reduction of transmittance.[11] Samples annealed at 1100 °C exhibited a significantly low sheet resistance of 5 kΩ sq^{-1} at 80% transmittance,[10] which is similar to our results. The data clearly show a consistent improvement in RGO film conductivity with $NaBH_4$ reduction. We emphasize here that the presence of C—N groups is the source of high sheet resistance in N_2H_4-reduced GO. Recently, a transparent conducting film was fabricated from dispersed graphene obtained by using exfoliated graphite,[12] as shown in Figure 5. The sheet resistance of this film was still higher than our result. After $NaBH_4$ reduction of GO, the film was further doped by $AuCl_3$. Sheet resistance consistently dropped by more than

Table 3. Electrical properties of the RGO films obtained using various concentrations of $NaBH_4$ and their related work functions.

	$NaBH_4$	XPS	Electrical Properties			UPS
		C:O ratio	Resistivity [Ωm]	Conductivity [S m^{-1}]	Sheet resistance [Ω sq^{-1}]	Work function [eV]
GO	–	2.2	1.5 E+7	6.8 E-8	–	–
RGO	15 mM	2.6	6.5 E+3	1.5 E-4	–	–
	50 mM	7.1	5.9 E-4	1.7 E+1	7.6 E+3	4.198
	150 mM	8.6	2.2 E-4	4.5 E+1	2.6 E+3	4.388
Graphite		72.5	–	1.0 E+3 ~ 1.4 E+5 [26]	–	4.400

Table 4. Percent transmittance (%T) at 550 nm and sheet resistance (R_s [kΩ sq^{-1}]) of RGO films in this study and other related studies.

Present work				Becerril et al. [10]				Eda et al. [11]				Li et al. [12]	
Reduced by $NaBH_4$		Reduced by $NaBH_4$ and Doped by $AuCl_3$		Reduced by N_2H_4 and annealed at 400 °C		Annealed at 1100 °C		Reduced by N_2H_4		Reduced by N_2H_4 and annealed at 200 °C		Dispersed Graphite	
%T	R_s	%T	R_s	%T	R_s	%T	R_s	%T	R_s	%T	R_s	%T	R_s
93.6	26.6	93.7	9.9					93.0	1000000				
91.2	22.6	91.3	9.1							90.0	1000	92.0	150.0
86.3	8.6	85.9	3.6									84.0	20.0
83.0	5.2	82.8	2.3					83.0	1500000				
81.0	4.4	80.8	2.1	80.0	50.0	80.0	5.0			80.0	100.0	79.0	8.0
77.9	2.8	76.8	1.4										
								73.0	20000				
										63.0	90.0		

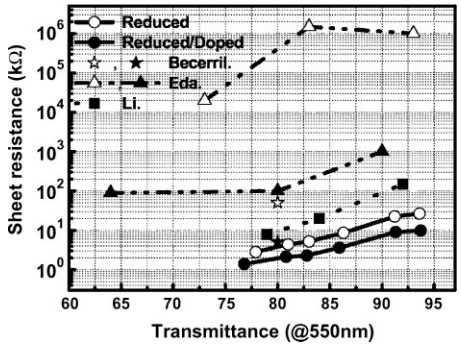

Figure 5. Sheet resistance versus transmittance at 550 nm for $NaBH_4$-reduced GO films before (open circles) and after (solid circles) Au-ion doping and N_2H_4-reduced GO films reported by others (Becirril, Eda, and Li correspond to references 10, 11, and 12, respectively).

50%, independent of the thickness of the film. Au^{3+} ions deposited onto the RGO extract electrons from the film, thus increasing hole carrier concentration. This phenomenon is similar to that of carbon nanotube doping.[27]

3. Conclusions

We have reported the effects of reducing agents on the sheet resistance of GO films. The sheet resistance of $NaBH_4$-reduced films was much lower than that of N_2H_4-reduced films exhibiting similar C–O composition. This result was attributed to the continuous accumulation of nitrogen atoms from hydrazine and the removal of oxygen atoms in the N_2H_4-reduced films. Nitrogen atoms behaved as donors compensating p-type hole carriers, which resulted in high sheet resistance when N_2H_4 was used as the reducing agent. We have investigated the underlying reduction mechanism of the alternative reducing agent, $NaBH_4$, and have studied the electrical properties in RGO films obtained using various concentrations of $NaBH_4$. The improved sheet resistance in $NaBH_4$-reduced GO films should open up more practical uses for RGOs.

4. Experimental

Synthesis and Dispersion of GOs: GOs were synthesized from pure graphite (99.999% purity, −200 mesh, Alfar Aesar) via a modified Brodie method [28]. Pure graphite (1 g) and sodium chlorate (8.5 g) were mixed in fuming nitric acid (20 mL) at room temperature without subsequent aging and stirred for up to 24 h. The following processes, such as washing, filtration, and cleaning, were carried out as in the Brodie method. The synthesized GO (10 mg) was dispersed in a aqueous NaOH solution (30 mL) at pH = 10. The prepared GO solution was sonicated in a bath-type sonicator (RK 106, Bandelin electronic, Germany) for 1 h at a power level of 240 W. After ultrasonication, samples were immediately precipitated by a centrifuge (4239R-V4, ALC International Srl, Italy) at 8000 rpm for 10 min. The stable supernatant solutions with well-dispersed GO was carefully extracted to make films.

Film Preparation and Reduction of GOs: GO films were prepared by spray equipment (NVD-200, Fujimori, Japan) using a specific volume of a dispersed GO solution on a polyethylene terephthalate (PET) substrate. To compare the effect of the reducing agents, $NaBH_4$ and N_2H_4, GO films were dipped in aqueous $NaBH_4$ (10 mM) and aqueous N_2H_4 (50 mM) solutions for various dipping times. In order to confirm the effect of the $NaBH_4$ reducing agent, GO films were dipped in $NaBH_4$ solutions of different concentrations (15, 50, and 150 mM) for 2 h.

Film Measurements and Electrical Characterization: The XPS spectrometer (QUANTUM 2000, Physical electronics, USA) was performed using focused monochromatized Al Kα radiation (1486.6 eV) in order to determine changes in the atomic ratios of carbon to oxygen and the existence of functional groups. The XPS spectra were fitted by using Multipak V6.1A software in which a Shirly background was assumed, and fitting the peaks of the experimental spectra were completed by considering a combination of Gaussian (80%) and Lorentzian (20%) distributions. The sheet resistance of the RGO films was measured by a four-point probe method (ChangMin, LTD, CMT-SR2000N, Korea). Powder XRD (D8 FOCUS 2.2 KW, Bruker AXS, Germany) with a Cu anode (1.54 Å) was used to measure the interlayer distance of the RGOs. Absorbance of RGO films was obtained by a UV-vis spectrometer (Varian Cary 5000, USA). Raman spectroscopy with an excitation energy of 1.96 eV (633 nm, Ar^+ ion laser) with a Rayleigh-line-rejection filter was used to study the defect formation. ^{13}C magic angle spinning (MAS) NMR spectra with ^1H decoupled spectra of GO, RGO (reduced using 150 mM of $NaBH_4$), and graphite were recorded on a Bruker

AVANCE III instrument (Germany) at 150.9 MHz and an MAS probe head with zirconia rotors 2.5 mm in diameter. The samples were spun in a 2.5 mm rotor at 15 kHz. Chemical shifts were calibrated indirectly through the glycine CO signal recorded at 176.0 ppm relative to tetramethylsilane (TMS). For XRD and Raman studies, GO films were formed directly on a Si wafer, and these films were reduced using the same method as that used for samples on PET. Metal electrodes were formed on the RGO/PET film to measure *I–V* characteristics. The electrode sources of Cr (50 Å) and Au (500 Å) were used. The width and length of a channel were 1000 and 100 μm, respectively. The work functions of the RGO films were measured by UPS (Gammadata VUV 5050, Sweden) using a HeI discharge lamp ($h\nu = 21.2$ eV). The work function was determined from the secondary electron cutoff of the UPS spectra using gold metal as a reference. The position of the Fermi level was calibrated by measuring the Fermi edge of the gold.

Preparation of Transparent Conducting Films: GO films were prepared on PET as indicated above, by controlling the volume of the dispersed GO solution. The films were reduced by dipping them in an aqueous $NaBH_4$ solution (150 mM) for 2 h. To remove excess $NaBH_4$, the RGO films were washed with water after reduction. A nitromethane solution of 15 μm $AuCl_3$ was spin-coated onto the RGO films at 2000 rpm for 30 s. Transmittance of the RGO films was measured using the Varian Cary UV-vis spectrometer, and their sheet resistance was measured again by four-point probe method.

Acknowledgements

This work was supported by the STAR-Faculty Project from MOEST, the KICOS through a grant provided by MOST (No. 2007-00202), and the KOSEF through CNNC at SKKU. Supporting Information is available online from Wiley InterScience or from the author.

Received: January 30, 2009
Published online: April 20, 2009

[1] S. Stankovich, D. A. Dikin, G. H. B. Dommett, K. M. Kohlhaas, E. J. Zimney, E. A. Stach, R. D. Piner, S. T. Nguyen, R. S. Ruoff, *Nature* **2006**, *442*, 282.
[2] H. C. Schniepp, J.-L. Li, M. J. McAllister, H. Sai, M. Herrera-Alonso, D. H. Adamson, R. K. Prud'homme, R. Car, D. A. Saville, I. A. Aksay, *J. Phys. Chem. B.* **2006**, *110*, 8535.
[3] M. J. McAllister, J.-L. Li, D. H. Adamson, H. C. Schniepp, A. A. Abdala, J. Liu, M. Herrera-Alonso, D. L. Milius, R. Car, R. K. Prud'homme, I. A. Aksay, *Chem. Mater.* **2007**, *19*, 4396.
[4] S. Stankovich, D. A. Dikin, R. D. Piner, K. A. Kohlhaas, A. Kleinhammes, Y. Jia, Y. Wu, S. T. Nguyen, R. S. Ruoff, *Carbon* **2007**, *45*, 1558.
[5] S. Stankovich, R. D. Piner, X. Chen, N. Wu, S. T. Nguyen, R. S. Ruoff, *J. Mater. Chem.* **2006**, *16*, 155.
[6] C. Gómez-Navarro, R. Thomas Weitz, A. M. Bittner, M. Scolari, A. Mews, M. Burghard, K. Kern, *Nano Lett.* **2007**, *7*, 3499.
[7] X. Wang, L. Zhi, K. Mullen, *Nano Lett.* **2008**, *8*, 323.
[8] S. Gilje, S. Han, M. Wang, K. L. Wang, R. B. Kaner, *Nano Lett.* **2007**, *7*, 3394.
[9] X. Fan, W. Peng, Y. Li, X. Li, S. Wang, G. Zhang, F. Zhang, *Adv. Mater.* **2008**, *20*, 4490.
[10] H. A. Becerril, J. Mao, Z. Liu, R. M. Stoltenberg, Z. Bao, Y. Chen, *ACS Nano* **2008**, *2*, 463.
[11] G. Eda, G. Fanchini, M. Chhowalla, *Nat. Nanotechnol.* **2008**, *3*, 270.
[12] X. Li, G. Zhang, X. Bai, X. Sun, X. Wang, E. Wang, H. Dai, *Nat. Nanotechnol.* **2008**, *3*, 538.
[13] a) N. Kishner, *J. Russ. Chem. Soc.* **1911**, *43*, 582. b) L. Wolff, *Liebigs Ann.* **1912**, *394*, 86.
[14] a) L. Banfi, E. Narisano, R. Riva, "Sodium Borohydride" in: *Encyclopedia of Reagents for Organic Synthesis* (Ed: L. Paquette), J. Wiley & Sons, New York **2004**. b) Y.-Q. Cao, Z. Dai, B.-H. Chen, R. Liu, *J. Chem. Tech. Biotechnol.* **2005**, *80*, 834.
[15] S . J Kang,, C. Kocabas, T. Ozel, M. Shim, N. Pimparkar, M. A. Alam, S. V. Rotkin, J. A. Rogers, *Nat. Nanotechnol.* **2007**, *2*, 230.
[16] J. Chen, C. Klinke, A. Afzali, K. Chan, P. Avouris, *IEDM Proceedings* **2004**, *4*, 895.
[17] M. Terrones, P. M. Ajayan, F. Banhart, X. Blase, D. L. Carroll, J. C. Charlier, R. Czerw, B. Foley, N. Grobert, R. Kamalakaran, P. Kohler-Redlich, M. Rühle, T. Seeger, H. Terrones, *Appl. Phys. A.* **2002**, *74*, 355.
[18] X. Li, X. Wang, L. Zhang, S. Lee, H. Dai, *Science* **2007**, *319*, 1129.
[19] K. S. Novoselov, A. K. Geim, S. V. Morozov, D. Jiang, Y. Zhang, S. V. Dubonos, I. V. Grigorieva, A. A. Science. Firsov, **2004**, *306*, 666.
[20] J.-H. Chen, C. Jang, S. Xiao, M. Ishigami, M. S. Fuhrer, *Nat. Nanotechnol.* **2008**, *3*, 206.
[21] H.-K. Jeong, Y. P. Lee, R. J. W. E. Lahaye, M.-H. Park, K. H. An, I. J. Kim, C.-W. Yang, C. Y. Park, R. S. Ruoff, Y. H. Lee, *J. Am. Chem. Soc.* **2008**, *130*, 1362.
[22] T. Szabo, O. Berkesi, P. Forgo, K. Josepovits, Y. Sanakis, D. Petridis, I. Dekany, *Chem. Mater.* **2006**, *18*, 2740.
[23] a) G. Beamson, D. Briggs, *High resolution XPS of Organic Polymers, The Scienta ESCA300 Database*, Wiley, Chichester, UK **1992**. b) J. F. Moudler, W. F. Stickle, P. E. Sobol, K. D. Bomben, *Handbook of X-ray Photoelectron Spectroscopy*, Perkin-Elmer, Eden Praitie, USA **1992**. c) J. A. Leiro, M. H. Heinonen, T. Laiho, I. G. Batirev, *J. Elec. Spec. Rela. Phen.* **2003**, *128*, 205.
[24] The GO compounds have slightly different ratios of functional groups from batch to batch, although C:O ratios were similar to each other. See, for instance, Fig. 2a and S1a in the Supporting Information.
[25] D. Li, M. B. Muller, S. Gilje, R. B. Kaner, G. G. Wallace, *Nat. Nanotechnol.* **2008**, *3*, 101.
[26] N. Deprez, D. S. McLachlan, *J. Phys. D: Appl. Phys.* **1998**, *21*, 101.
[27] K. K. Kim, J. J. Bae, H. K. Park, S. M. Kim, H.-Z. Geng, K. A. Park, H.-J. Shin, S.-M. Yoon, A. Benayad, J.-Y. Choi, Y. H. Lee, *J. Am. Chem. Soc.* **2008**, *130*, 12757.
[28] B. C. Brodie, *Ann. Chim. Phys.* **1860** *59*, 466.